

Dominant two-loop corrections to the MSSM finite temperature Effective Potential

J.R. Espinosa *

Deutsches Elektronen Synchrotron DESY.
Notkestrasse 85. 22603 Hamburg. Germany

Abstract

We show that two-loop corrections to the finite temperature effective potential in the MSSM can have a dramatic effect on the strength of the electroweak phase transition, making it more strongly first order. The change in the order parameter v/T_c can be as large as 75% of the one-loop daisy improved result. This effect can be decisive to widen the region in parameter space where erasure of the created baryons by sphaleron processes after the transition is suppressed and hence, where electroweak baryogenesis might be successful. We find an allowed region with $\tan\beta \lesssim 4.5$ and a Higgs boson with standard couplings and mass below 80 GeV within the reach of LEP II.

April 1996

*Work supported by the Alexander-von-Humboldt Stiftung.

1 Introduction

In recent years a considerable amount of work has been devoted to the study of the electroweak phase transition in the early Universe. A precise knowledge of it is crucial to determine if the very appealing idea of electroweak baryogenesis can be realized successfully at all (see [1] for review and references). It is by now clear that the minimal Standard Model (SM) has serious problems to generate a sufficient amount of baryon asymmetry at the electroweak phase transition. The needed CP violation is far too small and in addition the phase transition is at most weakly first order for realistic values of the Higgs boson mass. That is, the ratio v/T , of the (temperature dependent) vacuum expectation value (vev) for the scalar field and the temperature, is significantly smaller than 1 at the moment of the transition. Then, erasure of the created $B + L$ asymmetry by unsuppressed sphaleron transitions can not be prevented.

Nevertheless, electroweak baryogenesis may still be successful in alternative models. A particularly well motivated extension of the SM is the Minimal Supersymmetric Standard Model (MSSM) [2]. It admits additional sources of CP violation [3] and the presence of many extra particles in its spectrum can influence significantly the details of the electroweak phase transition. A careful study of that transition in this model (see [4, 5] for a study of the temperature dependent one-loop daisy improved potential and [6] for previous studies) has shown that (if all experimental constraints are appropriately taken into account) a strong enough first order phase transition ($v/T \gtrsim 1$) can only take place in a very small region of parameter space. That region corresponds to large pseudoscalar mass, $m_A \gg m_Z$, small $\tan \beta$ ($\sim 2 - 3$), third generation squarks as light as otherwise allowed and a SM-like Higgs boson with mass just above the present experimental limit ($m_h \gtrsim 64 \text{ GeV}$).

The purpose of this letter is to go beyond the one-loop daisy improved approximation for the finite temperature effective potential in the MSSM in order to see if the small window left for electroweak baryogenesis can be significantly widened. Similar studies, where the two-loop resummed potential is calculated, have been performed for the SM case [7] and sizeable corrections to different phase transition parameters were found. This in turn raised some doubts about the validity of perturbation theory and several alternative approaches were tried [8]. Focusing on $\mathcal{R} \simeq v(T_c)/T_c$ (T_c denotes the critical temperature, defined here by the coexistence of two degenerate minima in the potential), the quantity of interest for us, a careful comparison of two-loop resummed perturbative results and lattice simulations (see e.g. [9]) shows excellent agreement for moderate Higgs masses, indicating that perturbation theory is in better shape than previously thought. The inclusion of two-loop corrections tends to increase the value of $v(T_c)/T_c$ thus improving the prospects for preserving the baryon asymmetry against sphaleron erasure (although the improvement is not sufficient in the SM).

What can then be expected of a two-loop improvement for the MSSM? If the two-loop corrections turn out to be small, perturbation theory is trustworthy but the window for baryogenesis will remain marginal. If on the other hand very large corrections are found, perturbation theory will be suspect, and other techniques should be used. We hope to convince the reader that this is a naive expectation. We will show that large corrections

indeed appear, making the phase transition much stronger, and nevertheless perturbation theory could be still considered reliable and under control.

Before embarking on all the details, let us consider briefly what are the relevant expansion parameters in the problem and roughly estimate the size of the corrections expected. In the Standard Model the order of the phase transition is determined by transverse gauge bosons through its contribution to the cubic term in the effective potential (see [1] for details). The expansion parameter (in the minimum) can be identified as λ/g^2 , where λ is the quartic Higgs coupling and g the SU(2) gauge coupling. The requirement $\lambda/g^2 < 1$ then puts an upper limit to the Higgs mass region where perturbation theory can be trusted: roughly $m_h^2 \lesssim m_W^2$.

In the MSSM there are two main potential sources of differences with respect to the Standard Model: *i*) the presence of two Higgs doublets makes the effective potential a function of two background fields¹ and *ii*) contributions of supersymmetric particles to the effective potential can have an important effect on the transition. Concerning *i*), the two Higgs doublet potential is in fact tightly constrained by supersymmetry and it turns out that the best option for a strong transition corresponds to having only one light Higgs doublet (the case with a large pseudoscalar mass). Regarding the new contributions from supersymmetric particles it is easily realized that the key role is played by stops. If they are relatively light (of course, if all supersymmetric particles are heavy the Standard Model result for the corresponding Higgs mass is recovered) they drive the transition: being bosons, with a large number of degrees of freedom and sizeable coupling (h_t) to the Higgs field, they dominate the cubic term in the potential even if their thermal masses are of order $g_s T$.

In this situation the expansion parameter is λ/h_t^2 [11], where h_t is the top Yukawa coupling. Therefore the scale to determine whether the Higgs mass is too heavy to trust perturbation theory is set now by the top mass M_t while in the Standard Model it was set by M_W . This is just a naive estimate because the effect of the $g_s T$ screening can not be neglected and the coefficient in front of λ/h_t^2 that would give the proper expansion factor is unknown, but it suggests that perturbation theory can now be better behaved than it was in the SM for the same Higgs mass.

However, as we shall see, the situation in the MSSM is radically different from the SM case. It is not just a question of whether different effects will make the numerical coefficient in front of λ/h_t^2 large or small. The fact that squarks are *colored scalars* changes the picture completely: at two loops there are very important QCD corrections that affect $v(T_c)/T_c$ considerably and make the strong coupling g_s to appear directly in the game.

In the next section we review the one-loop daisy improved approximation for the MSSM potential [4, 5]. This will fix the notation and the interesting parameter range setting the stage for inclusion of two-loop dominant corrections, which will be the subject of section 3. Results and conclusion will be presented in sections 4 and 5 respectively. Some technical details are relegated to the appendices.

¹ Even barring the possibility that other MSSM scalars take non zero vevs at high temperatures one should allow for the possibility of a non-zero relative phase between the two Higgs vevs. This case was studied in refs. [10]. The region of parameter space where it can be realized is disconnected with the one which will interest us here.

2 One-loop resummed potential

We assume from the beginning that the pseudoscalar mass m_A is much larger than M_Z . In such case only one (combination) of the two Higgs doublets present in the MSSM is light. Then, the (light) physical Higgs boson has couplings to vector bosons and fermions of SM strength, and in first approximation the experimental limit $m_h \geq 64 \text{ GeV}$ applies. This simplifies the study of the potential which is then a function of just one background field as in the SM. From supersymmetric particles only squarks of the third generation will be considered to be at the electroweak scale. This corresponds to the best situation regarding the strength of the electroweak phase transition (see [4, 5] for more details). Our model reduces then to the SM plus third generation squarks and a quartic Higgs coupling fixed by supersymmetry as shown below.

Working in 't Hooft-Landau gauge and in $\overline{\text{MS}}$ -scheme², we can write the finite temperature effective potential in the form

$$V_{\text{eff}}(\varphi, T) = V_0(\varphi) + V_1(\varphi, 0) + \Delta V_1(\varphi, T) + \Delta V_{\text{daisy}}(\varphi, T), \quad (1)$$

where

$$V_0(\varphi) = -\frac{1}{2}\mu^2\varphi^2 + \frac{1}{32}\varphi^4(g^2 + g'^2)\cos^2 2\beta, \quad (2)$$

$$V_1(\varphi, 0) = \sum_i \frac{n_i}{64\pi^2} m_i^4(\varphi) \left[\log \frac{m_i^2(\varphi)}{Q^2} - C_i \right], \quad (3)$$

$$\Delta V_1(\varphi, T) = \frac{T^4}{2\pi^2} \sum_i n_i J_i \left[\frac{m_i^2(\varphi)}{T^2} \right], \quad (4)$$

$$\Delta V_{\text{daisy}}(\varphi, T) = -\frac{T}{12\pi} \sum_i n_i \left[\overline{m}_i^3(\varphi, T) - m_i^3(\varphi) \right]. \quad (5)$$

1) The first contribution, eq. (2), is just the tree level part. Note that the quartic Higgs coupling is fixed to be

$$\lambda = \frac{1}{8}(g^2 + g'^2)\cos^2 2\beta. \quad (6)$$

Here $\tan \beta$ is the ratio of the zero temperature vacuum expectation values of the two supersymmetric Higgses, $\langle H_2 \rangle / \langle H_1 \rangle = v_2 / v_1$, where H_2 is the doublet responsible for the masses of up-type quarks and $v_1^2 + v_2^2 = (246 \text{ GeV})^2$.

2) The second term, eq. (3), is the one-loop $T = 0$ contribution. Q is the renormalization scale, where we choose for definiteness $Q^2 = m_Z^2$. The n_i 's are the number of degrees of freedom of the different species of particles, taken negative for fermions:

$$n_t = -12, \quad n_{\tilde{t}_1} = n_{\tilde{t}_2} = 6, \quad n_W = 6, \quad n_Z = 3, \quad n_h = 1, \quad n_\chi = 3, \quad (7)$$

and C_i are constants equal to 5/6 for vector bosons, and 3/2 for scalars and fermions. The dominant piece of $V_1(\varphi, 0)$ comes from top and stop contributions.

²In refs. [4, 5] $\overline{\text{DR}}$ -scheme was used instead. We have checked that the numerical difference is irrelevant.

Next, $m_i(\varphi)$ is the field-dependent mass of the i^{th} particle. The field-dependent top and bottom masses are given by

$$m_t^2(\varphi) = \frac{1}{2}h_t^2\varphi^2 \sin^2 \beta \quad , \quad m_b^2(\varphi) = \frac{1}{2}h_b^2\varphi^2 \cos^2 \beta. \quad (8)$$

This implies the relations $h_{t,SM} = h_t \sin \beta$ and $h_{b,SM} = h_b \cos \beta$.

The entries of the field-dependent stop mass matrix are

$$m_{t_L}^2(\varphi) = m_Q^2 + m_t^2(\varphi) + D_{t_L}^2(\varphi), \quad (9)$$

$$m_{t_R}^2(\varphi) = m_U^2 + m_t^2(\varphi) + D_{t_R}^2(\varphi), \quad (10)$$

while the off-diagonal mixing between left and right-handed stops is given by

$$m_{t_{LR}}^2(\varphi) = \frac{h_t}{\sqrt{2}}(A_t \sin \beta + \mu \cos \beta)\varphi \equiv \frac{h_t}{\sqrt{2}}X_t\varphi. \quad (11)$$

Here m_Q , m_U and A_t are soft supersymmetry-breaking mass parameters³, μ is a superpotential Higgs mass term, and

$$D_{t_L}^2(\varphi) = \frac{1}{4} \left(\frac{1}{2} - \frac{2}{3} \sin^2 \theta_W \right) (g^2 + g'^2) \varphi^2 \cos 2\beta, \quad (12)$$

$$D_{t_R}^2(\varphi) = \frac{1}{4} \left(\frac{2}{3} \sin^2 \theta_W \right) (g^2 + g'^2) \varphi^2 \cos 2\beta, \quad (13)$$

are the D -term contributions to the stop mass matrix. The field-dependent stop masses, $m_{t_{1,2}}^2$, are the eigenvalues of the matrix described.

For sbottoms one has

$$m_{b_L}^2(\varphi) = m_Q^2 + m_b^2(\varphi) + D_{b_L}^2(\varphi), \quad (14)$$

$$m_{b_R}^2(\varphi) = m_D^2 + m_b^2(\varphi) + D_{b_R}^2(\varphi), \quad (15)$$

while the off-diagonal left-right mixing is now

$$m_{b_{LR}}^2(\varphi) = \frac{h_b}{\sqrt{2}}(A_b \cos \beta + \mu \sin \beta)\varphi \equiv \frac{h_b}{\sqrt{2}}X_b\varphi. \quad (16)$$

Here m_D , A_b are soft supersymmetry-breaking masses, and

$$D_{b_L}^2(\varphi) = \frac{1}{4} \left(-\frac{1}{2} + \frac{1}{3} \sin^2 \theta_W \right) (g^2 + g'^2) \varphi^2 \cos 2\beta, \quad (17)$$

$$D_{b_R}^2(\varphi) = \frac{1}{4} \left(-\frac{1}{3} \sin^2 \theta_W \right) (g^2 + g'^2) \varphi^2 \cos 2\beta. \quad (18)$$

The field-dependent masses for the gauge bosons are given by

$$m_W^2(\varphi) = \frac{1}{4}g^2\varphi^2, \quad m_Z^2(\varphi) = \frac{1}{4}(g^2 + g'^2)\varphi^2, \quad (19)$$

³For constraints on these parameters we refer the reader to the discussion in [4].

and for Higgs and Goldstone scalars by

$$m_h^2 = 3\lambda\varphi^2 - \mu^2, \quad m_{\chi_3^0}^2 = m_{\chi^\pm}^2 = \lambda\varphi^2 - \mu^2. \quad (20)$$

3) The third term in the potential, eq. (4), is the one-loop contribution due to temperature effects. Here $J_i = J_+(J_-)$ if the i^{th} particle is a boson (fermion), is the free energy of an ideal gas of particles of mass $m_i(\varphi)$,

$$J_\pm(y^2) = J_\pm(m^2/T^2) \equiv \int_0^\infty dx x^2 \log \left(1 \mp e^{-\sqrt{x^2+y^2}} \right). \quad (21)$$

4) The last term, eq. (5), is a correction coming from the resummation of the leading infrared-dominated higher-loop contributions, associated with the so-called daisy diagrams. The sum runs over bosons only. The effect of this contribution is to replace the pure cubic term $m^3(\varphi)$ that arises from (4) by $\overline{m}^3(\varphi)$. The masses $\overline{m}_i^2(\varphi, T)$ are obtained from the $m_i^2(\varphi)$ by adding⁴ the leading T -dependent self-energy contributions, which are proportional to T^2 . We recall that, in the gauge boson sector, only the longitudinal components (W_L, Z_L, γ_L) receive such contributions⁵. Also note

$$n_{W_L} = 2, \quad n_{Z_L} = n_{\gamma_L} = 1. \quad (22)$$

The (leading order) thermal polarizations for different particles can be found in ref. [4] and are reproduced in appendix A together with some extra polarizations needed for two-loop corrections to the potential. We assume here that only SM particles and third generation squarks contribute to these thermal masses, the rest being heavy and decoupled. As explained in [4] this is the best case for a strong first order transition and in practice corresponds to the case of heavy gluinos, so that the results found can be interpreted as the best guess for a realistic supersymmetric spectrum.

The contribution of stops to ΔV_{daisy} is responsible for the enhancement of $\mathcal{R} = v(T_c)/T_c$ with respect to the SM result. The final region in parameter space where $\mathcal{R} > 1$ is determined by the interplay between different opposite effects: soft and thermal screening masses tend to decrease \mathcal{R} by screening the pure cubic behaviour of $m_t^3(\varphi)$ while a large Yukawa coupling (thus a large top mass) tend to increase it. For a given value of h_t (and $\tan\beta$) there is a minimum allowed value of m_Q [the constraint of $\Delta\rho$ on the mass splitting of the $(\tilde{t}, \tilde{b})_L$ doublet gets weaker for larger m_Q] and this will correspond to the best case. To determine which of the competing effects is stronger one has to study numerically the potential as was done in [4, 5]. The main conclusion of those papers is that in some regions of parameter space the cubic term from stops is effective and actually dominates the electroweak phase transition.

Regions of $\mathcal{R} > 1$ can be found for $135 \text{ GeV} \lesssim M_t \lesssim 170 \text{ GeV}$. The best case always corresponds to negligible mixing in the stop mass matrix ($m_{tLR}^2 \sim 0$), low $\tan\beta$ ($\sim 2 - 3$),

⁴In general, \overline{m}_i^2 will be the eigenvalues of the corresponding mass matrix after addition of thermal contributions.

⁵Longitudinal photons do contribute to the effective potential due to the effect described in the previous footnote.

a Higgs mass close to the experimental limit ($m_h \leq 70 \text{ GeV}$) and squarks of the third generation as light as allowed by the $\Delta\rho$ constraint.

To fix ideas, for $m_t = 150 \text{ GeV}$ (which corresponds to a physical pole mass $M_t = 156 \text{ GeV}$), $m_Q = 70 \text{ GeV}$ [this gives $\Delta\rho(t, b) + \Delta\rho(\tilde{t}_L, \tilde{b}_L) < 0.01$], $m_U = m_{\tilde{t}_{LR}} = 0$ and $\tan\beta = 2.5$, $v(T_c)/T_c = 1.02$ and so this point in parameter space corresponds roughly to the border of the $\mathcal{R} > 1$ area. The Higgs mass is $\sim 65 \text{ GeV}$.

3 Two-loop resummed potential

The complete two-loop resummed potential for the contributions of SM particles can be found in refs. [7]. Regarding its effect on the quantity $\mathcal{R} = v(T_c)/T_c$, the most important corrections are those coming from bosonic setting sun diagrams, which cause logarithms of masses to appear. The importance of these contributions was first pointed out by Bagnasco and Dine in [7]. In particular, the most important effect is due to logarithms of transverse vector boson masses, unscreened at leading order. It is enough for our purpose to keep only logarithmic SM terms. We will also set $g' = 0$ for all two-loop corrections. This will simplify the analytic results being numerically an excellent approximation. In addition we will use throughout a high temperature expansion keeping contributions to the effective potential up to order g^4 (where for power counting g represents gauge, Yukawa couplings or $\sqrt{\lambda}$). In our formulas, M will represent the (field-dependent) weak vector boson mass and M_L the longitudinal, Debye-screened mass (see appendix A):

$$M^2 = \frac{1}{4}g^2\varphi^2, \quad M_L^2 = M^2 + \frac{7}{3}g^2T^2. \quad (23)$$

Then, the dominant two-loop resummed SM piece of the potential can be written as

$$V_{SM}^{(2)} = \frac{g^2}{16\pi^2}T^2 \left[M^2 \left(\frac{3}{4} \log \frac{M_L}{T} - \frac{51}{8} \log \frac{M}{T} \right) + \frac{3}{2}(M^2 - 4M_L^2) \log \frac{M + 2M_L}{3T} \right]. \quad (24)$$

Some comments are in order. Extra logarithmic contributions involving scalar (Higgs) masses have been systematically neglected (although these were also kept for the numerical analysis). That is a good approximation because near the critical temperature their effective mass is small. We have kept logarithms of longitudinal vector boson masses [note that only the $\log(M/T)$ was kept in Bagnasco and Dine paper]. They are not important numerically because the screening of gauge bosons is very effective here but we keep them for consistency: similar logarithms will appear for the supersymmetric contribution. Terms like the last one in (24) have a linear dependence on φ for small field. As is well known, this linear dependence cancels when all resummed two-loop contributions are kept. We shall then add the terms needed to insure this cancellation here. These are [7]

$$\delta V_{SM}^{(2)} = \frac{3g^2}{16\pi^2}MM_L T^2. \quad (25)$$

There are also non logarithmic contributions involving g_s and h_t that can be sizeable in principle. They are [7]:

$$\delta'V_{SM}^{(2)} = \frac{m_t^2(\varphi)T^2}{64\pi^2} \left[16g_s^2 \left(\frac{8}{3} \log 2 - \frac{1}{2} - c_B \right) + 9h_{t,SM}^2 \left(\frac{4}{3} \log 2 - c_B \right) \right]. \quad (26)$$

Here, the constant c_B is given by

$$c_B = \log(4\pi) - \gamma_E \quad (27)$$

where γ_E is Euler's constant. This correction affects mainly the numerical value of the critical temperature while its effect on \mathcal{R} is very small.

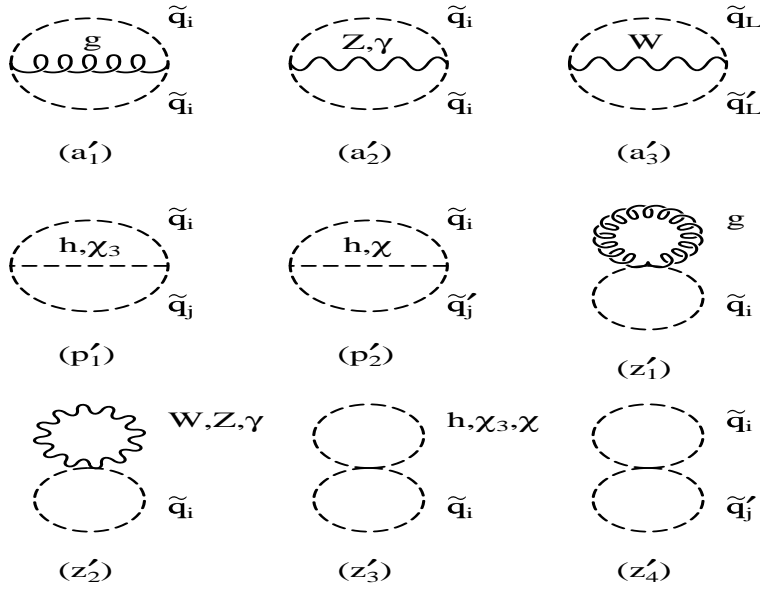


Figure 1: Two-loop graphs involving third generation squarks.

The extra supersymmetric diagrams⁶ we have to consider are depicted in figure 1. Note that, with our assumptions on the supersymmetric spectrum, R-parity conservation implies that squarks appear always in closed loops. Furthermore, there are no fermionic diagrams because all $R = -1$ fermions are assumed heavy (two-loop diagrams with e.g. a top quark and a stop involve also higgsinos or gluinos to close the fermion loop). We label the diagrams in a similar way as in refs. [7]. By \tilde{q}_i we represent a squark of a given flavour q and chirality $i = L, R$. Then, \tilde{q}'_j would stand for a squark of different flavour and different chirality.

The dominant logarithmic contribution (plus linear terms) can then be written, in the high temperature expansion (see appendix B for the integral expression), as the sum of the following pieces ($N_c = 3$ is the number of colours):

$$V_{(a'_1)} = -\frac{g_s^2(N_c^2 - 1)T^2}{16\pi^2} \left[\bar{m}_{\tilde{t}_L}^2 \log \frac{2\bar{m}_{\tilde{t}_L}}{3T} + \bar{m}_{\tilde{t}_R}^2 \log \frac{2\bar{m}_{\tilde{t}_R}}{3T} + \bar{m}_{\tilde{b}_L}^2 \log \frac{2\bar{m}_{\tilde{b}_L}}{3T} \right], \quad (28)$$

⁶For MSSM Feynman rules see e.g. [12].

$$\begin{aligned}
V_{(a'_{2,3})} &= \frac{g^2 N_c T^2}{32\pi^2} \left[-\frac{3M}{2} (\overline{m}_{\tilde{t}_L} + \overline{m}_{\tilde{b}_L}) \right. \\
&+ \frac{1}{4} (M^2 - 4\overline{m}_{\tilde{t}_L}^2) \log \frac{M + 2\overline{m}_{\tilde{t}_L}}{3T} + \frac{1}{4} (M^2 - 4\overline{m}_{\tilde{b}_L}^2) \log \frac{M + 2\overline{m}_{\tilde{b}_L}}{3T} \\
&+ \left. [M^2 - 2(\overline{m}_{\tilde{t}_L}^2 + \overline{m}_{\tilde{b}_L}^2)] \log \frac{M + \overline{m}_{\tilde{t}_L} + \overline{m}_{\tilde{b}_L}}{3T} + \frac{(\overline{m}_{\tilde{t}_L}^2 - \overline{m}_{\tilde{b}_L}^2)^2}{M^2} \log \frac{M + \overline{m}_{\tilde{t}_L} + \overline{m}_{\tilde{b}_L}}{\overline{m}_{\tilde{t}_L} + \overline{m}_{\tilde{b}_L}} \right], \tag{29}
\end{aligned}$$

$$\begin{aligned}
V_{(p'_{1,2})} &= \frac{N_c \varphi^2 T^2}{32\pi^2} \left[\left(h_{t,SM}^2 + \frac{1}{4} g^2 \cos 2\beta \right)^2 \log \frac{\overline{m}_h + 2\overline{m}_{\tilde{t}_L}}{3T} + \left(h_{t,SM}^2 \right)^2 \log \frac{\overline{m}_h + 2\overline{m}_{\tilde{t}_R}}{3T} \right. \\
&+ \left. \left(h_{t,SM}^2 + \frac{1}{2} g^2 \cos 2\beta \right)^2 \log \frac{\overline{m}_\chi + \overline{m}_{\tilde{t}_L} + \overline{m}_{\tilde{b}_L}}{3T} + \left(\frac{1}{4} g^2 \cos 2\beta \right)^2 \log \frac{\overline{m}_h + 2\overline{m}_{\tilde{b}_L}}{3T} \right]. \tag{30}
\end{aligned}$$

In this last contribution we are neglecting stop mixing ($m_{\tilde{t}_{LR}} \sim 0$). As was shown in [4, 5] for the one-loop potential, this is the best case to maximize \mathcal{R} . The two-loop resummed potential for non-zero stop mixing can be found in appendix C.

The (z') diagrams do not contribute logarithmic terms but they are needed to cancel the linear dependence present in the previous pieces:

$$V_{(z')} = \frac{3g^2}{32\pi^2} N_c T^2 M (\overline{m}_{\tilde{t}_L} + \overline{m}_{\tilde{b}_L}). \tag{31}$$

From the rest of non logarithmic terms we will keep those involving g_s^2 and h_t^2 only:

$$\begin{aligned}
\delta V_{(a'_1)} &= -\frac{g_s^2 T^2}{64\pi^2} (N_c^2 - 1) (c_2 - 1) (\overline{m}_{\tilde{t}_L}^2 + \overline{m}_{\tilde{t}_R}^2), \\
\delta V_{(p'_{1,2})} &= \frac{3N_c}{128\pi^2} T^2 h_{t,SM}^4 c_2 \varphi^2, \\
\delta V_{(z'_{1,2})} &= \frac{g_s^2 T^2}{32\pi^2} (N_c^2 - 1) \left[\Pi_{gL}^{1/2} (\overline{m}_{\tilde{t}_L} + \overline{m}_{\tilde{t}_R}) + \frac{1}{6} (\overline{m}_{\tilde{t}_L}^2 + \overline{m}_{\tilde{t}_R}^2) \right] + \delta_{c_B} V_{(z'_{1,2})}, \\
\delta V_{(z'_{3,4})} &= \frac{N_c T^2}{16\pi^2} \left[\frac{g_s^2}{6} (N_c + 1) (\overline{m}_{\tilde{t}_L}^2 + \overline{m}_{\tilde{t}_R}^2) + h_t^2 \overline{m}_{\tilde{t}_R} (\overline{m}_{\tilde{t}_L} + \overline{m}_{\tilde{b}_L}) \right. \\
&+ \left. \frac{1}{2} h_{t,SM}^2 (\overline{m}_h (\overline{m}_{\tilde{t}_L} + \overline{m}_{\tilde{t}_R}) + \overline{m}_\chi (\overline{m}_{\tilde{t}_L} + 3\overline{m}_{\tilde{t}_R})) \right] + \delta_{c_B} V_{(z'_{3,4})}, \tag{32}
\end{aligned}$$

where $c_2 \simeq 3.3025$. Here Π_{gL} is the Debye mass for longitudinal gluons as given in appendix A. We have neglected throughout the bottom Yukawa coupling, which is small for small $\tan \beta$. Then terms dependent on $\overline{m}_{\tilde{b}_R}$ are not shown.

The complete terms $\delta_{c_B} V$ add up to give

$$\frac{c_B}{16\pi^2} \left[6 \sum_i m_{\tilde{q}_i}^2 \Pi_{\tilde{q}_i}^{SUSY} + m_h^2 \Pi_h^{SUSY} + 3m_\chi^2 \Pi_\chi^{SUSY} \right]. \tag{33}$$

As expected, this term plus a similar term from Standard Model polarizations, combines with the one-loop unresummed scalar contribution

$$\frac{c_B}{32\pi^2} \sum_i n_i m_i^4, \tag{34}$$

to give the same result but with $m_i \rightarrow \bar{m}_i$ (a welcome check of the calculation). In (33) $\Pi_i^{SU\mathcal{S}Y}$ is the full thermal mass for squarks while for the Higgs modes it includes only the contribution of supersymmetric particles (see appendix A):

$$\Pi_h^{SU\mathcal{S}Y} = \Pi_\chi^{SU\mathcal{S}Y} = \frac{1}{2}h_t^2 \sin^2 \beta T^2. \quad (35)$$

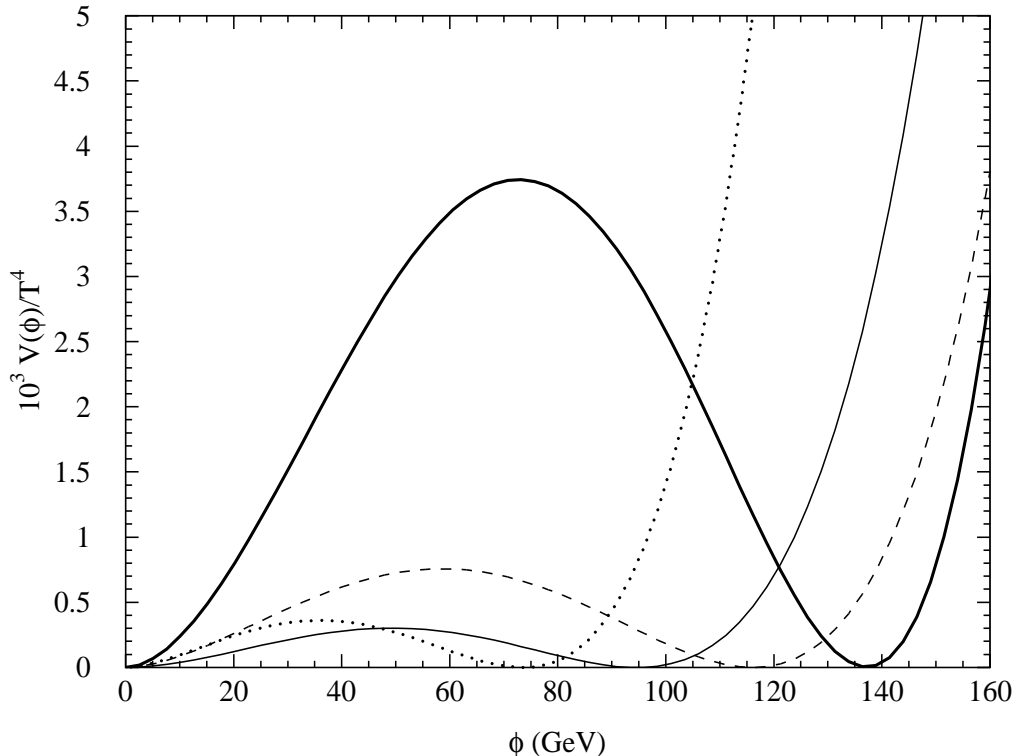


Figure 2: Scaled potential at the critical temperature for different approximations: one-loop resummed potential (thin solid line); potential with two-loop resummed contributions from SM particles only (dashed); with two-loop resummed supersymmetric non-QCD contributions added (dotted); with all dominant two-loop resummed contributions (thick solid). [$M_t = 156 \text{ GeV}$, $m_Q = 70 \text{ GeV}$, $m_U = m_{\bar{t}_{LR}} = 0$ and $\tan \beta = 2.5$].

4 Results

In figure 2, different approximations to the scaled effective potential $[V(\varphi)/T^4]$ are plotted at the corresponding critical temperature. Parameters are fixed as in the example at the end of section 2: top pole mass $M_t = 156 \text{ GeV}$, $m_Q = 70 \text{ GeV}$, $m_U = m_{\bar{t}_{LR}} = 0$ and $\tan \beta = 2.5$. The thin solid line corresponds to the one-loop resummed potential for which $\mathcal{R} = 1.02$. The effect of including two-loop corrections from Standard Model particles is shown by the dashed line: the transition becomes stronger and \mathcal{R} increases up to 1.20. This effect can be traced back [7] to the presence of corrections of the form $-\varphi^2 \log \varphi$ coming from transverse

gauge boson modes [see eq. (24)]. A contribution of this form has a direct effect shifting the value of the vev at the critical temperature. The minus sign in front implies that the shift is towards larger values. To examine two-loop corrections from supersymmetric particles it is convenient to split them in two categories: QCD contributions and the rest. Looking first at non QCD terms, the dominant effect [see eqs. (28-32)] is of the form $+\varphi^2 \log \bar{\varphi}$ (where $\bar{\varphi}$ represents some screened masses). The net positive sign indicates that these corrections contribute to make the phase transition weaker. This effect can be seen in figure 2 where the dotted line includes non QCD squark contributions. The corresponding \mathcal{R} falls now down to 0.97, slightly below the one-loop resummed result. Then, disregarding QCD corrections, the convergence of the perturbative series for \mathcal{R} seems to be much better in the supersymmetric case, when the phase transition is driven by squarks, than in the Standard Model (for the same Higgs mass).

The inclusion of QCD corrections changes completely this picture: a look at (28) reveals that these corrections are of the form $-\varphi^2 \log \bar{\varphi}$ and sizeable, implying that \mathcal{R} will be shifted to larger values. The increase in \mathcal{R} can be as dramatic as shown in figure 2. The thick solid line gives the scaled potential with all dominant corrections included. The phase transition in this approximation is much stronger and $\mathcal{R} = 1.75$ (a correction of 75% over the one-loop result!).

This huge effect makes perturbative validity dubious. Nevertheless, one should keep in mind that the effect is very large because QCD corrections appear only at two loops (the same happens in the Standard Model but there, the effect is associated with a fermionic loop and so the final effect on \mathcal{R} is much less important) and not at one-loop⁷. Then, a large ratio of the two-loop to the one-loop result does not necessarily imply that perturbation theory is not applicable. To settle definitively this issue one should estimate the size of three-loop corrections. However, that is beyond the aim of this paper. Note also that lattice simulations would face here the problem that squarks carry color so that $SU(3)_c$ can no longer be ignored as in the SM once fermions were integrated out. Lacking an estimate of higher order corrections, certainly this two-loop result indicates that the transition is probably much stronger than what the one-loop resummed approximation indicated.

In the previous numerical example we have chosen the parameters to maximize the effect on \mathcal{R} . We explore now how \mathcal{R} changes when we move in parameter space. Figure 3 is a contour plot of \mathcal{R} (solid lines) in the plane $(m_U, \tan \beta)$ for $m_t = 150 \text{ GeV}$ ($M_t = 156 \text{ GeV}$) and $m_Q = 70 \text{ GeV}$. The dashed lines give the Higgs boson mass⁸ m_h in GeV. Thick lines are used to single out the lines $\mathcal{R} = 1$ and $m_h = 64 \text{ GeV}$. The region where electroweak baryogenesis could in principle be viable and the LEP I bound on m_h evaded is now sizeable. Values of $\tan \beta$ larger than in the one-loop case are allowed and Higgs masses up to $\sim 80 \text{ GeV}$ can be reached. The decrease of \mathcal{R} with increasing m_U is just the effect of a growing screening in $\bar{m}_{\tilde{t}_R}$. For large values of m_U the high temperature expansion breaks down and one should

⁷This situation is by no means unique and appears in many other cases. Similar examples can be found already in the MSSM Higgs sector, e.g. when considering radiative corrections to the mass of the lightest scalar [13] or QCD radiative corrections to hadronic Higgs decays [15].

⁸To compute the Higgs mass accurately is important to include loop corrections which can be sizeable [13, 14].

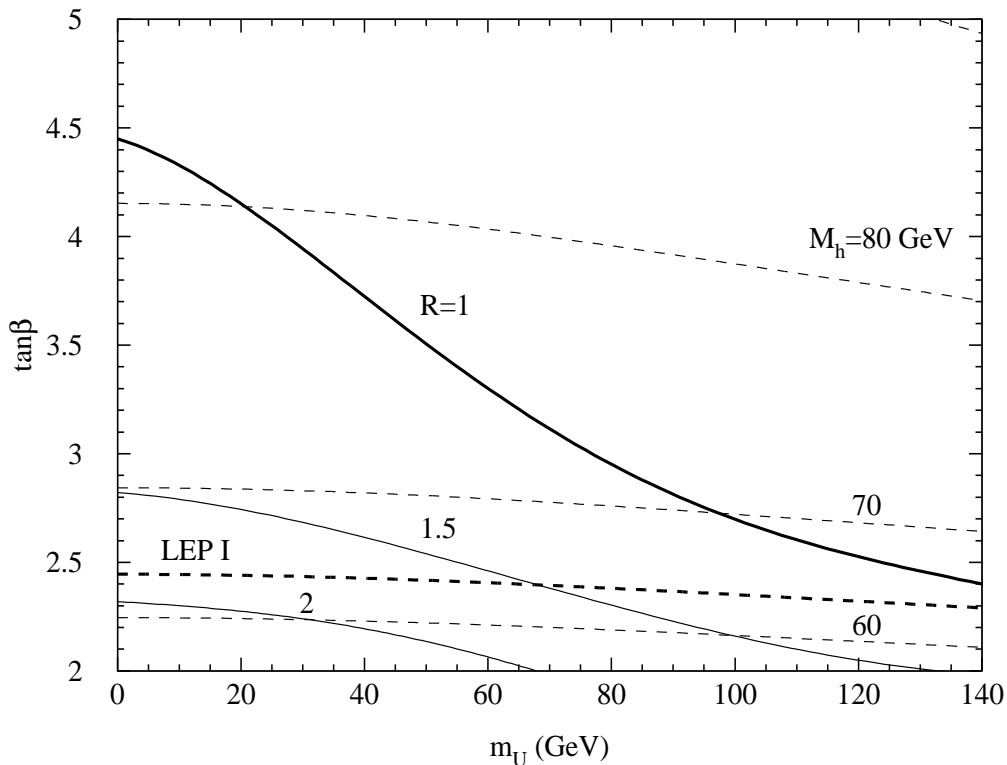


Figure 3: Contour lines of \mathcal{R} (solid) and m_h (dashed) in the $(m_U, \tan \beta)$ plane for $M_t = 156 \text{ GeV}$ and $m_Q = 70 \text{ GeV}$.

evaluate two-loop contributions numerically. We cut the x-axis for $m_U = 140 \text{ GeV}$ where the high T expansion is still safe.

Finally, figure 4 shows contour lines of constant \mathcal{R} and m_h in the plane $(M_t, \tan \beta)$. Thick solid lines for $\mathcal{R} = 1$ and $m_h = 64 \text{ GeV}$ delimit a "baryogenesis hole" where the electroweak phase transition is strong and the lightest Higgs mass is above the LEP I limit. The region corresponds to $125 \text{ GeV} \leq M_t \leq 185 \text{ GeV}$ and $\tan \beta \leq 4.5$. In this plot we have set $m_U = 0$ and m_Q has been fixed at its lowest value such that the constraint on $\Delta\rho$ is evaded (fixing for simplicity $\tan \beta = 2$ to compute this minimum of m_Q). The range of m_Q then varies from zero for $M_t = 120 \text{ GeV}$ to order 1 TeV for $M_t = 180 \text{ GeV}$. The dependence of \mathcal{R} contours on M_t is then easy to understand: for low values of M_t the effect of squarks is smaller because the Yukawa coupling is smaller. In this region, increasing M_t one gets larger values of \mathcal{R} . For larger M_t , two effects collaborate to change this tendency. Large M_t requires large m_Q to avoid problems with $\Delta\rho$ so that left-handed squarks are required to be heavy. In turn, heavy squarks give a sizeable radiative correction to the Higgs mass making it heavier and correspondingly decreasing the strength of the transition. This is purely a zero temperature effect. For the finite temperature corrections, heavy left-handed squarks are in fact decoupled and do not contribute: \mathcal{R} in this region has been calculated with contributions of right handed squarks only. Therefore, the effect is reduced and \mathcal{R} drops. The net effect is that one ends up with a closed region in the $(M_t, \tan \beta)$ plane where

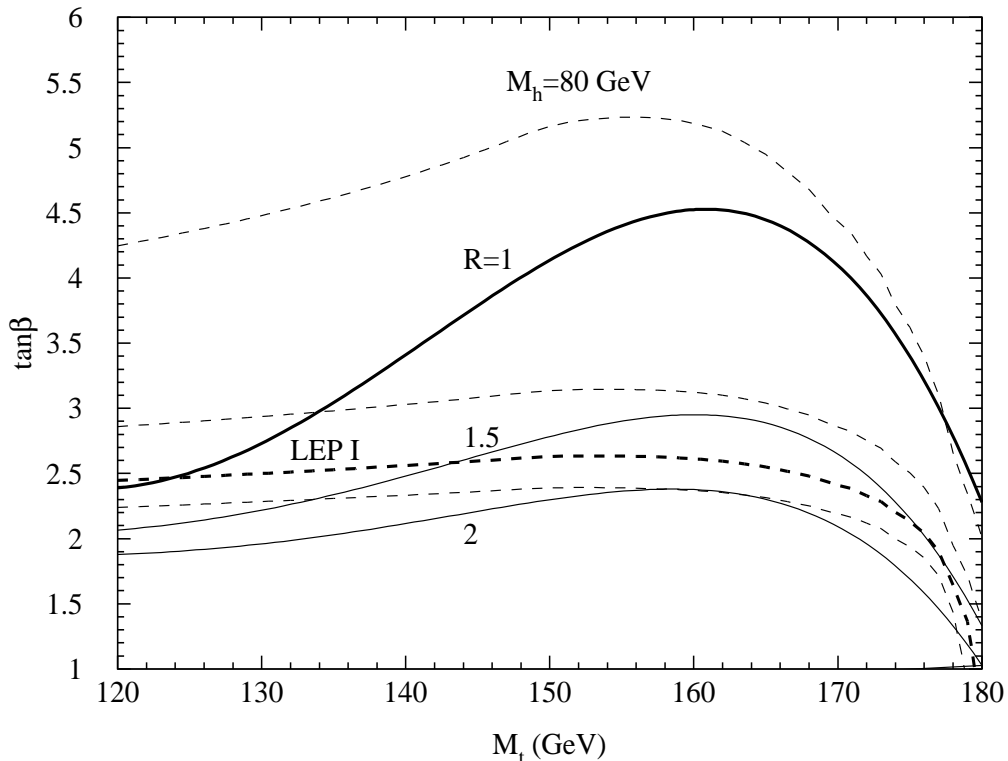


Figure 4: Contour lines of \mathcal{R} (solid) and m_h (dashed) in the $(M_t, \tan\beta)$ plane for $m_U = 0$ and m_Q above the limit to avoid the $\Delta\rho$ constraint.

electroweak baryogenesis may be successful. It is interesting to note that this region requires large M_t in a range compatible with the CDF-D0 range. Furthermore m_h is bounded to be below ~ 80 GeV so that LEP II will scan this "baryogenesis hole" in the near future testing then one of the crucial ingredients for the viability of electroweak baryogenesis in the MSSM.

5 Conclusion

In the MSSM light stops can dominate completely the electroweak phase transition in the early Universe. We have shown that the strength of this transition is dramatically affected by QCD corrections that first appear at two-loop order. They make the transition strongly first order in some non marginal region of parameter space compatible with experimental constraints. This is in sharp contrast with the situation in the Standard Model where transverse gauge bosons drive the transition which is weak for realistic Higgs masses.

The allowed region found corresponds to $\tan\beta$ small within a reasonable range ($\tan\beta \lesssim 4.5$), squarks as light as allowed by electroweak precision constraints and only one light Higgs boson, with Standard couplings and mass as large as 80 GeV. Such Higgs scalar is within the reach of LEP II so that these region will be explored in the forthcoming years.

The sizeable increase in the strength of the electroweak phase transition can be decisive to open the window for electroweak baryogenesis in the MSSM and should encourage further

studies of many different aspects of the problem [17] still not well understood and necessary towards a complete mechanism of electroweak (supersymmetric) baryogenesis.

Note Added

In a very recent paper [16] the electroweak phase transition in the MSSM is studied in the previously unexplored case $m_U^2 < 0$ which is shown to be phenomenologically allowed. In such region of parameter space the screening of $\overline{m}_{\tilde{t}_R}$ is then reduced and \mathcal{R} can be larger than 1 even at one-loop. Then the allowed areas found in the present paper can be continued into the $m_U^2 < 0$ region improving further the prospects for supersymmetric electroweak baryogenesis.

Acknowledgements

Thanks go to A. Brignole, W. Buchmüller, M. Cacciari, M. Carena, A. Hebecker, M. Quiros, J. Rosiek, M. Spira, C. Wagner and F. Zwirner for useful comments, discussions, and suggestions regarding different aspects of this work.

Appendix A

We reproduce here the leading parts of the T-dependent self energies for the different species of bosonic particles. Most of these results were presented in ref. [4]. Some errata are corrected now (see Ref.[18] for details). It is assumed that m_A is large so that only one light Higgs doublet is present at the electroweak scale. The second doublet is decoupled and does not contribute to the thermal polarizations written below. As in ref. [4] terms outside curly brackets come from Standard Model contributions and third generation squarks. The rest of the supersymmetric contributions is inside the brackets and is written for completeness.

Note that, at leading order, these thermal masses are equal for particles inside the same $SU(2)$ multiplet. They are given by

$$\begin{aligned}
\Pi_{W_L} &= \frac{7}{3}g^2T^2 + \{2g^2T^2\}, \\
\Pi_{B_L} &= \frac{22}{9}g'^2T^2 + \left\{\frac{26}{9}g'^2T^2\right\}, \\
\Pi_h &= \Pi_\chi = \frac{1}{16}(g^2 + g'^2) \cos^2 2\beta T^2 + \frac{3}{16}g^2T^2 + \frac{1}{16}g'^2T^2 + \frac{3}{4}h_t^2 \sin^2 \beta T^2 \\
&\quad + \left\{\frac{1}{8}g^2T^2 + \frac{1}{24}g'^2T^2\right\}, \\
\Pi_{\tilde{t}_L} &= \Pi_{\tilde{b}_L} = \frac{4}{9}g_s^2T^2 + \frac{1}{4}g^2T^2 + \frac{1}{216}g'^2(2 - 3 \cos 2\beta)T^2 + \frac{1}{12}h_t^2(1 + \sin^2 \beta)T^2 \\
&\quad + \left\{\frac{2}{9}g_s^2T^2 + \frac{1}{8}g^2T^2 + \frac{1}{216}g'^2T^2 + \frac{1}{12}h_t^2T^2\right\},
\end{aligned}$$

$$\begin{aligned}
\Pi_{\tilde{t}_R} &= \frac{4}{9}g_s^2T^2 + \frac{1}{54}g'^2(8 + 3\cos 2\beta)T^2 + \frac{1}{6}h_t^2(1 + \sin^2\beta)T^2 \\
&+ \left\{ \frac{2}{9}g_s^2T^2 + \frac{2}{27}g'^2T^2 + \frac{1}{6}h_t^2T^2 \right\}, \\
\Pi_{\tilde{b}_R} &= \frac{4}{9}g_s^2T^2 + \frac{1}{108}g'^2(4 - 3\cos 2\beta)T^2 + \left\{ \frac{2}{9}g_s^2T^2 + \frac{1}{54}g'^2T^2 \right\}.
\end{aligned}$$

We complete these formulae giving the polarization for longitudinal gluons

$$\Pi_{g_L} = \frac{8}{3}g_s^2T^2 + \left\{ \frac{11}{6}g_s^2T^2 \right\}.$$

This last result is needed for a two-loop calculation of the effective potential.

Appendix B

We write here the resummed supersymmetric two-loop corrections to the finite temperature effective potential in the MSSM framework described in the text. In particular we consider $g' = h_b = 0$ so that in the formulas below we make no distinction between m_Z and m_W which are called M . We assume also that left-right mixing in the stop sector is negligible. Our notation is that of Arnold and Espinosa in [7] and the labelling of different contributions corresponds to our figure 1. As usual, $N_c = 3$ counts the number of colours.

$$\begin{aligned}
V_{(a')} &= -\frac{g^2}{8}N_c \left[\mathcal{D}_{SSV}(m_{\tilde{t}_L}, m_{\tilde{t}_L}, M) + \mathcal{D}_{SSV}(m_{\tilde{b}_L}, m_{\tilde{b}_L}, M) + 4\mathcal{D}_{SSV}(m_{\tilde{t}_L}, m_{\tilde{b}_L}, M) \right] \\
&- \frac{g_s^2}{4}(N_c^2 - 1) \left[\mathcal{D}_{SSV}(m_{\tilde{t}_L}, m_{\tilde{t}_L}, 0) + \mathcal{D}_{SSV}(m_{\tilde{b}_L}, m_{\tilde{b}_L}, 0) \right. \\
&+ \left. \mathcal{D}_{SSV}(m_{\tilde{t}_R}, m_{\tilde{t}_R}, 0) + \mathcal{D}_{SSV}(m_{\tilde{b}_R}, m_{\tilde{b}_R}, 0) \right], \\
V_{(p')} &= - \left[\left(h_t^2 \sin^2\beta + \frac{g^2}{4} \cos 2\beta \right)^2 \bar{\mathbb{H}}(m_h, m_{\tilde{t}_L}, m_{\tilde{t}_L}) + \left(\frac{g^2}{4} \cos 2\beta \right)^2 \bar{\mathbb{H}}(m_h, m_{\tilde{b}_L}, m_{\tilde{b}_L}) \right. \\
&+ \left. (h_t^2 \sin^2\beta)^2 \bar{\mathbb{H}}(m_h, m_{\tilde{t}_R}, m_{\tilde{t}_R}) + \left(h_t^2 \sin^2\beta + \frac{1}{2}g^2 \cos 2\beta \right)^2 \bar{\mathbb{H}}(m_h, m_{\tilde{t}_L}, m_{\tilde{b}_L}) \right] \frac{\varphi^2}{2} N_c, \\
V_{(z'_{1,2})} &= -\frac{1}{4}g_s^2(N_c^2 - 1) \left[\mathcal{D}_{SV}(m_{\tilde{t}_L}, 0) + \mathcal{D}_{SV}(m_{\tilde{b}_L}, 0) + \mathcal{D}_{SV}(m_{\tilde{t}_R}, 0) + \mathcal{D}_{SV}(m_{\tilde{b}_R}, 0) \right] \\
&- \frac{3}{8}g^2N_c \left[\mathcal{D}_{SV}(m_{\tilde{t}_L}, M) + \mathcal{D}_{SV}(m_{\tilde{b}_L}, M) \right], \\
V_{(z'_{3,4})} &= \frac{g^2}{4}N_c(2 - N_c)\mathcal{D}_S(m_{\tilde{t}_L}, m_{\tilde{b}_L}) + h_t^2N_c \left[\mathcal{D}_S(m_{\tilde{t}_L}, m_{\tilde{t}_R}) + \mathcal{D}_S(m_{\tilde{b}_L}, m_{\tilde{t}_R}) \right] \\
&+ \left(\frac{g^2}{8} + \frac{g_s^2}{6} \right) N_c(N_c + 1) \left[\mathcal{D}_S(m_{\tilde{t}_L}, m_{\tilde{t}_L}) + \mathcal{D}_S(m_{\tilde{b}_L}, m_{\tilde{b}_L}) \right]
\end{aligned}$$

$$\begin{aligned}
& + \frac{g_s^2}{6} N_c(N_c + 1) \left[\mathcal{D}_S(m_{\tilde{t}_R}, m_{\tilde{t}_R}) + \mathcal{D}_S(m_{\tilde{b}_R}, m_{\tilde{b}_R}) \right] \\
& + N_c \left(\frac{1}{2} h_t^2 \sin^2 \beta + \frac{1}{8} g^2 \cos 2\beta \right) \left[\mathcal{D}_S(m_{\tilde{t}_L}, m_h) + 2\mathcal{D}_S(m_{\tilde{b}_L}, m_\chi) + \mathcal{D}_S(m_{\tilde{t}_L}, m_\chi) \right] \\
& - \frac{1}{8} N_c g^2 \cos 2\beta \left[\mathcal{D}_S(m_{\tilde{b}_L}, m_h) + 2\mathcal{D}_S(m_{\tilde{t}_L}, m_\chi) + \mathcal{D}_S(m_{\tilde{b}_L}, m_\chi) \right] \\
& + \frac{1}{2} N_c h_t^2 \sin^2 \beta \left[\mathcal{D}_S(m_{\tilde{t}_R}, m_h) + 2\mathcal{D}_S(m_{\tilde{t}_R}, m_\chi) + \mathcal{D}_S(m_{\tilde{t}_R}, m_\chi) \right],
\end{aligned}$$

where $\mathcal{D}_S(m_1, m_2)$ is simply the resummed version of

$$\mathcal{D}_S^{\not{R}}(m_1, m_2) = I(m_1)I(m_2).$$

In the previous formulae, dimensional regularization (with $n - 1 = 3 - 2\epsilon$) is used to evaluate divergent integrals. Poles in $1/\epsilon$ and ν_ϵ -dependent terms cancel when counterterms are included. In addition, counterterms contribute a finite piece to the potential [7]. To compute the finite piece due to third generation squarks note that the counterterm potential can be written now as

$$\begin{aligned}
\delta V & = \frac{1}{2} \varphi^2 \left\{ -\mu^2 (\delta Z_{\mu^2} + \delta Z_{\varphi^2}) + I_\beta^\epsilon \left[6\lambda (\delta Z_\lambda + \delta Z_{\varphi^2}) + 6h_{t,SM}^2 (\delta Z_{h_{t,SM}^2} + \delta Z_{\varphi^2}) \right. \right. \\
& + \left. \left. \frac{1}{4} (3 - 2\epsilon) \left(3g^2 (\delta Z_{g^2} + \delta Z_{\varphi^2}) + g'^2 (\delta Z_{g'^2} + \delta Z_{\varphi^2}) \right) \right] - 6h_{t,SM}^2 I_{f\beta}^\epsilon (\delta Z_{h_{t,SM}^2} + \delta Z_{\varphi^2}) \right\} \\
& + \frac{\lambda}{8} \varphi^4 (\delta Z_\lambda + \delta Z_{\varphi^2}), \tag{36}
\end{aligned}$$

with

$$I_\beta^\epsilon = \frac{T^2}{12} (1 + \epsilon \nu_\epsilon) \quad , \quad I_{f\beta}^\epsilon = -\frac{T^2}{24} [1 + \epsilon (\nu_\epsilon - \log 4)].$$

The $\overline{\text{MS}}$ renormalization functions δZ have no finite part, so the finite (ν_ϵ -independent) piece of δV is given by the $(3 - 2\epsilon)$ and $I_{f\beta}^\epsilon$ terms. The required contributions of third generation squarks to the renormalization functions are

$$\delta_{\tilde{q}_3} Z_{g^2} = \frac{1}{2} g^2 \frac{1}{16\pi^2 \epsilon}, \quad \delta_{\tilde{q}_3} Z_{g'^2} = \frac{11}{18} g'^2 \frac{1}{16\pi^2 \epsilon}, \quad \delta_{\tilde{q}_3} Z_{\varphi^2} = \delta_{\tilde{q}_3} Z_{h_{t,SM}^2} = 0. \tag{37}$$

The third equation follows from the fact that squarks are scalars while the fourth is a consequence of our assumptions about the supersymmetric spectrum, that has no light $R = -1$ fermions. The finite contribution is then

$$\delta V = -\frac{T^2}{16\pi^2} \frac{\varphi^2}{96} \left(3g^4 + \frac{11}{9} g'^4 \right). \tag{38}$$

Appendix C

To include the effect of the left-right squark mixing appropriate mixing angles, α_t for stops and α_b for sbottoms, should be defined. When temperature corrections are included in the mass matrix for the zero Matsubara modes, the corresponding mixing angles will turn out to be temperature dependent. This effect has to be taken into account when writing the resummed effective potential and zero modes should be treated independently. It is then possible to generalize the previous expression for the effective potential writing it in terms of unresummed \mathcal{D} 's plus extra terms for the resummation of zero modes. A similar situation arises with the photon-Z mixing in the Standard Model. In the same way that this complication is circumvented in the Standard Model just by setting $g' = 0$, a reasonable assumption for the squark case would be to approximate the squark thermal masses by its universal QCD contribution $4g_s^2 T^2/9$ and neglect the rest. In this way the thermal correction to the squared mass matrices would be diagonal and the mixing angles would be temperature independent. In this approximation, the generalization of the previous expression for the potential is straightforward. Writing

$$\begin{cases} \tilde{t}_1 = \cos \alpha_t \tilde{t}_L + \sin \alpha_t \tilde{t}_R & \tilde{b}_1 = \cos \alpha_b \tilde{b}_L + \sin \alpha_b \tilde{b}_R \\ \tilde{t}_2 = \cos \alpha_t \tilde{t}_R - \sin \alpha_t \tilde{t}_L & \tilde{b}_2 = \cos \alpha_b \tilde{b}_R - \sin \alpha_b \tilde{b}_L \end{cases} \quad (39)$$

we obtain (using the abbreviations $c_t = \cos \alpha_t$, $c_{2\beta} = \cos 2\beta$, etc)

$$\begin{aligned} V_{(a')} &= -\frac{g^2}{8} N_c \left[c_t^4 \mathcal{D}_{SSV}(m_{\tilde{t}_1}, m_{\tilde{t}_1}, M) + s_t^4 \mathcal{D}_{SSV}(m_{\tilde{t}_2}, m_{\tilde{t}_2}, M) + 2c_t^2 s_t^2 \mathcal{D}_{SSV}(m_{\tilde{t}_1}, m_{\tilde{t}_2}, M) \right] \\ &- \frac{g^2}{8} N_c \left[c_b^4 \mathcal{D}_{SSV}(m_{\tilde{b}_1}, m_{\tilde{b}_1}, M) + s_b^4 \mathcal{D}_{SSV}(m_{\tilde{b}_2}, m_{\tilde{b}_2}, M) + 2c_b^2 s_b^2 \mathcal{D}_{SSV}(m_{\tilde{b}_1}, m_{\tilde{b}_2}, M) \right] \\ &- \frac{g^2}{2} N_c \left[c_t^2 c_b^2 \mathcal{D}_{SSV}(m_{\tilde{t}_1}, m_{\tilde{b}_1}, M) + s_t^2 s_b^2 \mathcal{D}_{SSV}(m_{\tilde{t}_2}, m_{\tilde{b}_2}, M) + c_t^2 s_b^2 \mathcal{D}_{SSV}(m_{\tilde{t}_1}, m_{\tilde{b}_2}, M) \right. \\ &+ \left. s_t^2 c_b^2 \mathcal{D}_{SSV}(m_{\tilde{t}_2}, m_{\tilde{b}_1}, M) \right] - \frac{g_s^2}{4} (N_c - 1) \left[\mathcal{D}_{SSV}(m_{\tilde{t}_1}, m_{\tilde{t}_1}, 0) + \mathcal{D}_{SSV}(m_{\tilde{b}_1}, m_{\tilde{b}_1}, 0) \right. \\ &+ \left. \mathcal{D}_{SSV}(m_{\tilde{t}_2}, m_{\tilde{t}_2}, 0) + \mathcal{D}_{SSV}(m_{\tilde{b}_2}, m_{\tilde{b}_2}, 0) \right], \end{aligned}$$

$$\begin{aligned} V_{(p')} &= -\frac{N_c}{2} \left\{ 2 \left[\frac{g^2}{4} \varphi c_t s_t c_{2\beta} + \frac{h_t}{\sqrt{2}} (A_t s_\beta + \mu c_\beta) c_{2t} \right]^2 \bar{\mathbb{H}}(m_h, m_{\tilde{t}_1}, m_{\tilde{t}_2}) \right. \\ &+ \left[(h_t^2 s_\beta^2 + \frac{g^2}{4} c_t^2 c_{2\beta}) \varphi - h_t \sqrt{2} (A_t s_\beta + \mu c_\beta) c_t s_t \right]^2 \bar{\mathbb{H}}(m_h, m_{\tilde{t}_1}, m_{\tilde{t}_1}) \\ &+ \left. \left[(h_t^2 s_\beta^2 + \frac{g^2}{4} s_t^2 c_{2\beta}) \varphi + h_t \sqrt{2} (A_t s_\beta + \mu c_\beta) c_t s_t \right]^2 \bar{\mathbb{H}}(m_h, m_{\tilde{t}_2}, m_{\tilde{t}_2}) \right\} \\ &- \frac{N_c}{2} \left\{ 2 \left[\frac{g^2}{4} \varphi c_b s_b c_{2\beta} + \frac{h_b}{\sqrt{2}} (A_b c_\beta + \mu s_\beta) c_{2b} \right]^2 \bar{\mathbb{H}}(m_h, m_{\tilde{b}_1}, m_{\tilde{b}_2}) \right. \\ &+ \left[(h_b^2 c_\beta^2 + \frac{g^2}{4} c_b^2 c_{2\beta}) \varphi - h_b \sqrt{2} (A_b c_\beta + \mu s_\beta) c_b s_b \right]^2 \bar{\mathbb{H}}(m_h, m_{\tilde{b}_1}, m_{\tilde{b}_1}) \\ &+ \left. \left[(h_b^2 c_\beta^2 + \frac{g^2}{4} s_b^2 c_{2\beta}) \varphi + h_b \sqrt{2} (A_b c_\beta + \mu s_\beta) c_b s_b \right]^2 \bar{\mathbb{H}}(m_h, m_{\tilde{b}_2}, m_{\tilde{b}_2}) \right\} \end{aligned}$$

$$\begin{aligned}
& + \left[\frac{g^2}{4} \varphi c_b^2 c_{2\beta} - h_b \sqrt{2} (A_b c_\beta + \mu s_\beta) c_b s_b \right]^2 \bar{\mathbb{H}}(m_h, m_{\tilde{b}_1}, m_{\tilde{b}_1}) \\
& + \left[\frac{g^2}{4} \varphi s_b^2 c_{2\beta} + h_b \sqrt{2} (A_b c_\beta + \mu s_\beta) c_b s_b \right]^2 \bar{\mathbb{H}}(m_h, m_{\tilde{b}_2}, m_{\tilde{b}_2}) \Big\} \\
& - \frac{N_c}{2} \varphi^2 \left(\frac{g^2}{4} c_{2\beta} \right)^2 \left[c_b^4 \bar{\mathbb{H}}(m_h, m_{\tilde{b}_1}, m_{\tilde{b}_1}) + s_b^4 \bar{\mathbb{H}}(m_h, m_{\tilde{b}_2}, m_{\tilde{b}_2}) + 2c_b^2 s_b^2 \bar{\mathbb{H}}(m_h, m_{\tilde{b}_1}, m_{\tilde{b}_2}) \right] \\
& - \frac{N_c}{2} \left[h_t^2 (A_t s_\beta + \mu c_\beta)^2 \bar{\mathbb{H}}(m_\chi, m_{\tilde{t}_1}, m_{\tilde{t}_2}) + h_b^2 (A_b c_\beta + \mu s_\beta)^2 \bar{\mathbb{H}}(m_\chi, m_{\tilde{b}_1}, m_{\tilde{b}_2}) \right] \\
& - N_c \left\{ \left[\frac{\varphi}{\sqrt{2}} (h_t^2 s_\beta^2 + \frac{g^2}{2} c_{2\beta}) c_t c_b + h_t X_t s_t c_b - h_b X_b c_t s_b \right]^2 \bar{\mathbb{H}}(m_\chi, m_{\tilde{t}_1}, m_{\tilde{b}_1}) \right. \\
& + \left[\frac{\varphi}{\sqrt{2}} (h_t^2 s_\beta^2 + \frac{g^2}{2} c_{2\beta}) c_t s_b + h_t X_t s_t s_b + h_b X_b c_t c_b \right]^2 \bar{\mathbb{H}}(m_\chi, m_{\tilde{t}_1}, m_{\tilde{b}_2}) \\
& + \left[\frac{\varphi}{\sqrt{2}} (h_t^2 s_\beta^2 + \frac{g^2}{2} c_{2\beta}) s_t c_b - h_t X_t c_t c_b - h_b X_b s_t s_b \right]^2 \bar{\mathbb{H}}(m_\chi, m_{\tilde{t}_2}, m_{\tilde{b}_1}) \\
& \left. + \left[\frac{\varphi}{\sqrt{2}} (h_t^2 s_\beta^2 + \frac{g^2}{2} c_{2\beta}) s_t s_b - h_t X_t c_t s_b + h_b X_b s_t c_b \right]^2 \bar{\mathbb{H}}(m_\chi, m_{\tilde{t}_2}, m_{\tilde{b}_2}) \right\},
\end{aligned}$$

where we keep h_b only when it appears in combination with X_b .

$$\begin{aligned}
V_{(z'_{1,2})} & = -\frac{1}{4} g_s^2 (N_c^2 - 1) \left[\mathcal{D}_{SV}(m_{\tilde{t}_1}, 0) + \mathcal{D}_{SV}(m_{\tilde{b}_1}, 0) + \mathcal{D}_{SV}(m_{\tilde{t}_2}, 0) + \mathcal{D}_{SV}(m_{\tilde{b}_2}, 0) \right] \\
& - \frac{3}{8} g^2 N_c \left[c_t^2 \mathcal{D}_{SV}(m_{\tilde{t}_1}, M) + s_t^2 \mathcal{D}_{SV}(m_{\tilde{t}_2}, M) + c_b^2 \mathcal{D}_{SV}(m_{\tilde{b}_1}, M) + s_b^2 \mathcal{D}_{SV}(m_{\tilde{b}_2}, M) \right],
\end{aligned}$$

$$\begin{aligned}
V_{(z'_{3,4})} & = \frac{g_s^2}{6} N_c (N_c + 1) \left[\mathcal{D}_S(m_{\tilde{t}_1}, m_{\tilde{t}_1}) + \mathcal{D}_S(m_{\tilde{b}_1}, m_{\tilde{b}_1}) + \mathcal{D}_S(m_{\tilde{t}_2}, m_{\tilde{t}_2}) \right. \\
& + \left. \mathcal{D}_S(m_{\tilde{b}_2}, m_{\tilde{b}_2}) \right] + \frac{N_c}{2} \left[\left(h_t^2 s_\beta^2 + \frac{g^2}{4} c_t^2 c_{2\beta} \right) \left[\mathcal{D}_S(m_h, m_{\tilde{t}_1}) + \mathcal{D}_S(m_\chi, m_{\tilde{t}_1}) \right] \right. \\
& + \left. \left(h_t^2 s_\beta^2 + \frac{g^2}{4} s_t^2 c_{2\beta} \right) \left[\mathcal{D}_S(m_h, m_{\tilde{t}_2}) + \mathcal{D}_S(m_\chi, m_{\tilde{t}_2}) \right] \right] + N_c h_t^2 \left[c_b^2 s_t^2 \mathcal{D}_S(m_{\tilde{b}_1}, m_{\tilde{t}_1}) \right. \\
& + \left. c_b^2 c_t^2 \mathcal{D}_S(m_{\tilde{b}_1}, m_{\tilde{t}_2}) + s_b^2 s_t^2 \mathcal{D}_S(m_{\tilde{b}_2}, m_{\tilde{t}_1}) + s_b^2 c_t^2 \mathcal{D}_S(m_{\tilde{b}_2}, m_{\tilde{t}_2}) \right] \\
& - \frac{N_c g^2 c_{2\beta}}{8} \left[c_b^2 \left[\mathcal{D}_S(m_h, m_{\tilde{b}_1}) - \mathcal{D}_S(m_\chi, m_{\tilde{b}_1}) \right] + s_b^2 \left[\mathcal{D}_S(m_h, m_{\tilde{b}_2}) - \mathcal{D}_S(m_\chi, m_{\tilde{b}_2}) \right] \right. \\
& + \left. 2c_t^2 \mathcal{D}_S(m_\chi, m_{\tilde{t}_1}) + 2s_t^2 \mathcal{D}_S(m_\chi, m_{\tilde{t}_2}) \right] \\
& + N_c h_t^2 s_\beta^2 \left[s_t^2 \mathcal{D}_S(m_\chi, m_{\tilde{t}_1}) + c_t^2 \mathcal{D}_S(m_\chi, m_{\tilde{t}_2}) + c_b^2 \mathcal{D}_S(m_\chi, m_{\tilde{b}_1}) + s_b^2 \mathcal{D}_S(m_\chi, m_{\tilde{b}_2}) \right] \\
& + N_c h_t^2 c_t^2 s_t^2 \left[(N_c + 1) \left[\mathcal{D}_S(m_{\tilde{t}_1}, m_{\tilde{t}_1}) + \mathcal{D}_S(m_{\tilde{t}_2}, m_{\tilde{t}_2}) \right] - 2N_c c_t^2 s_t^2 \mathcal{D}_S(m_{\tilde{t}_1}, m_{\tilde{t}_2}) \right] \\
& + \frac{g^2}{4} N_c (2 - N_c) \left[c_t^2 c_b^2 \mathcal{D}_S(m_{\tilde{t}_1}, m_{\tilde{b}_1}) + c_t^2 s_b^2 \mathcal{D}_S(m_{\tilde{t}_1}, m_{\tilde{b}_2}) + s_t^2 c_b^2 \mathcal{D}_S(m_{\tilde{t}_2}, m_{\tilde{b}_1}) \right.
\end{aligned}$$

$$\begin{aligned}
& + s_t^2 s_b^2 \mathcal{D}_S(m_{\tilde{t}_2}, m_{\tilde{b}_2}) \Big] + N_c h_t^2 (c_t^4 + s_t^4) \mathcal{D}_S(m_{\tilde{t}_1}, m_{\tilde{t}_2}) \\
& + \frac{1}{8} g^2 N_c (N_c + 1) \left[c_t^4 \mathcal{D}_S(m_{\tilde{t}_1}, m_{\tilde{t}_1}) + 2c_t^2 s_t^2 \mathcal{D}_S(m_{\tilde{t}_1}, m_{\tilde{t}_2}) + s_t^4 \mathcal{D}_S(m_{\tilde{t}_2}, m_{\tilde{t}_2}) \right] \\
& + \frac{1}{8} g^2 N_c (N_c + 1) \left[c_b^4 \mathcal{D}_S(m_{\tilde{b}_1}, m_{\tilde{b}_1}) + 2c_b^2 s_b^2 \mathcal{D}_S(m_{\tilde{b}_1}, m_{\tilde{b}_2}) + s_b^4 \mathcal{D}_S(m_{\tilde{b}_2}, m_{\tilde{b}_2}) \right].
\end{aligned}$$

References

- [1] A.G. Cohen, D.B. Kaplan and A.E. Nelson, *Ann. Rev. Nucl. Part. Sci.* 43 (1993) 27;
V.A. Rubakov and M.E. Shaposhnikov, Preprint CERN-TH/96-13 [hep-ph/9603208].
- [2] See e.g. H.P. Nilles, *Phys. Rep.* 110 (1984) 1;
H.E. Haber and G.L. Kane, *Phys. Rep.* 117 (1985) 75;
M. Drees and S.P. Martin, Preprint MADPH-95-879 [hep-ph/9504324];
H. Baer et al. Preprint FSU-HEP-950401 [hep-ph/9503479].
- [3] J. Ellis, S. Ferrara and D.V. Nanopoulos, *Phys. Lett.* B114 (1982) 231;
W. Buchmüller and D. Wyler, *Phys. Lett.* B121 (1983) 321;
J. Polchinski and M.B. Wise, *Phys. Lett.* B125 (1983) 393;
F. del Aguila, B. Gavela, J. Grifols and A. Mendez, *Phys. Lett.* B126 (1983) 71;
D.V. Nanopoulos and M. Srednicki, *Phys. Lett.* B128 (1983) 61;
M. Dugan, B. Grinstein and L.J. Hall, *Nucl. Phys.* B255 (1985) 413.
- [4] J.R. Espinosa, M. Quirós and F. Zwirner, *Phys. Lett.* B307 (1993) 106.
- [5] A. Brignole, J.R. Espinosa, M. Quirós and F. Zwirner, *Phys. Lett.* B324 (1994) 181.
- [6] G.F. Giudice, *Phys. Rev.* D45 (1992) 3177;
S. Myint, *Phys. Lett.* B287 (1992) 325.
- [7] J.E. Bagnasco and M. Dine, *Phys. Lett.* B303 (1993) 308;
P. Arnold and O. Espinosa, *Phys. Rev.* D47 (1993) 3546; ERRATUM-ibid. D50 (1994) 6662.
Z. Fodor and A. Hebecker, *Nucl. Phys.* B432 (1994) 127;
W. Buchmüller, Z. Fodor, A. Hebecker, *Nucl. Phys.* B447 (1995) 317;
K. Farakos, K. Kajantie, K. Rummukainen and M. Shaposhnikov, *Nucl. Phys.* B425 (1994) 67.
- [8] See e. g. L.G. Yaffe, [hep-ph/9512265] for references.
- [9] K. Jansen, DESY Preprint DESY 95-169, [hep-lat/9509018] and references therein.
- [10] D. Comelli and M. Pietroni, *Phys. Lett.* B306 (1993) 67;
D. Comelli, M. Pietroni and A. Riotto, *Nucl. Phys.* B412 (1994) 441;
J.R. Espinosa, J.M. Moreno and M. Quirós, *Phys. Lett.* B319 (1993) 505.

- [11] J.R. Espinosa, in: Electroweak Physics and the Early Universe, NATO ASI Series B: Physics Vol. 338, p.93. (Edts. J.C. Romao and F. Freire) Plenum Press 1994.
- [12] J. Rosiek, Phys. Rev. D41 (1990) 3464; Erratum: Preprint KA-TP-8-1995 [hep-ph/9511250].
- [13] Y. Okada, M. Yamaguchi and T. Yanagida, Prog. Theor. Phys. Lett. 85 (1991) 1 and Phys. Lett. B262 (1991) 54;
 J. Ellis, G. Ridolfi and F. Zwirner, Phys. Lett. B257 (1991) 83;
 H.E. Haber and R. Hempfling, Phys. Rev. Lett. 66 (1991) 1815;
 R. Barbieri and M. Frigeni, Phys. Lett. B258 (1991) 395.
- [14] R. Hempfling and H. Hoang, Phys. Lett. B331 (1994) 99;
 J. Kodaira, Y. Yasui and K. Sasaki, Phys. Rev. D50 (1994) 7035;
 J.A. Casas, J.R. Espinosa, M. Quirós and A. Riotto, Nucl. Phys. B436 (1995) 3;
 M. Carena, J.R. Espinosa, M. Quirós and C.E.M. Wagner, Phys. Lett. B335 (1995) 209;
 M. Carena, M. Quirós and C.E.M. Wagner, Nucl. Phys. B461 (1996) 407;
 H.E. Haber, R. Hempfling and H. Hoang, Preprint CERN-TH/95-216.
- [15] A. Djouadi, M. Spira and P.M. Zerwas, Preprint DESY 95-210 [hep-ph/9511344].
- [16] M. Carena, M. Quirós and C.E.M. Wagner, CERN Preprint CERN-TH/96-30 [hep-ph/9603420].
- [17] P. Huet and A. Nelson, Phys. Lett. B355 (1995) 229; Phys. Rev. D53 (1996) 4578;
 D. Comelli, M. Pietroni and A. Riotto, Phys. Lett. B354 (1995) 91; Phys. Rev. D53 (1996) 4668;
 A. Riotto, Preprint SISSA-117-95-AP [hep-ph/9510271] to appear in Phys. Rev. D.
- [18] D. Comelli and J.R. Espinosa, DESY Preprint to appear.